Estd. 1989
Asian Journal of Chemistry; Vol. 23, No. 9 (2011), 3853-3858
ASIAN JOURNAL OF CHEMISTRY
www.asianjournalofchemistry.co.in

$VOPO_4 \cdot 2H_2O$ and The Vanadium Phosphate Catalyst Produced by Sonochemical Synthesis

Y.C. WONG[1,2*] and Y.H. TAUFIQ-YAP[2,3]

[1]Faculty of Agro Industry and Natural Resources, Universiti Malaysia Kelantan, Locked Bag 36, Pengkalan Chepa, 16100 Kota Bharu, Kelantan Darul Naim, Malaysia.
[2]Centre of Excellence for Catalysis Science and Technology, Universiti Putra Malaysia, 43400 UPM Serdang, Selangor Darul Ehsan, Malaysia
[3]Department of Chemistry, Faculty of Science, Universiti Putra Malaysia, 43400 UPM Serdang, Selangor Darul Ehsan, Malaysia

*Corresponding author: Fax: +609 771 7232; Tel: +609 771 7087; E-mail: yeeching@umk.edu.my

(*Received*: 20 August 2010; *Accepted*: 9 May 2011) AJC-9920

Six vanadyl phosphate dihydrate were prepared *via* sonochemical synthesis with different duration of time, *i.e.* 15, 30, 45, 60, 90 and 120 min are denoted as DS15, DS30, DS45, DS60, DS90 and DS120, respectively. DS120 were chosen as starting material to further proceed to form VPO catalyst through conventional reflux method. The synthesized materials were characterized by X-ray diffraction (XRD), scanning electron microscope (SEM), transmission electron microscope (TEM) and temperature-programmed reduction (TPR) in H_2. Catalytic evaluation of the sonochemical treated VPO catalyst, VPDS120 was also studied on microreactor. From the XRD patterns of the vanadyl phosphate dihydrate obtained, $VOPO_4 \cdot 2H_2O$, *via* sonochemical synthesis in different duration of time are perfectly matched with the standard $VOPO_4 \cdot 2H_2O$, indicating the high purity of the $VOPO_4 \cdot 2H_2O$ produced through this sonochemical synthesis technique that have been drastically reduced the synthesis time to only 15 min compared to the conventional reflux method that consumed the synthesis time up to 24 h. VPDS120 catalyst shows a drastically increment in the percentage of *n*-butane conversion compared to conventional VPD catalyst. This phenomenon occurred majorly due to the VPDS120 catalyst produced has smaller diameters and thickness of platelets that directly increase the active site of the catalyst for oxidation of *n*-butane. Furthermore, VPDS120 catalyst contain more V^{4+} percentage which also directly lead to the increment of the total amount of active and mobile oxygen attached to V^{4+} phase (O^{-}-V^{4+} pair).

Key Words: Sonochemical synthesis, Vanadyl phosphate dihydrate, Butane oxidation.

INTRODUCTION

Despite several studies worldwide, progress in sonochemical synthesis has been hampered by low *n*-butane conversion and serious catalyst deactivation due to coke formation. It is well known that the preparation method of catalyst can affect the channel structure, the acid site density and the oxidation state and location of the vanadium species. These factors are recognized to affect the catalytic performance of *n*-butane conversion. Thus, this leads to the investigation of new preparation method and to the further optimization of catalyst performance.

By using ultrasound irradiation, it is believed that it can enhanced the chemical reaction and mass transfer *via* the process of acoustic cavitation which relatively shorten the time of VPO catalyst preparation while still displays comparable oxidation activity for the liquid phase hydrogen peroxide oxidation of cycloalkanes in acetonitrile[1]. In this study, the physico-chemical properties of the vanadyl pyrophosphate catalysts synthesized *via* sonochemical synthesis and its starting materials (vanadyl phosphate dihydrate) were characterized by using X-ray diffraction (XRD), chemical analysis, scanning electron microscope (SEM), transmission electron microscope (TEM) and temperature-programmed reduction (H_2-TPR). Catalytic oxidation of *n*-butane was also carried out to evaluate the catalytic behaviour of the VPO catalysts produced.

EXPERIMENTAL

Preparation of sonochemical synthesis of $VOPO_4 \cdot 2H_2O$: Vanadium pentoxide (2 g from Fluka), orthophosphoric acid (32 mL, 85 % from Merck) and 100 mL of distilled water were mixed in 250 mL beaker and exposed to high intensity irradiation under ambient air for 15, 30, 45, 60, 90 and 120 min. Ultrasound irradiation was accomplished with a high intensity ultrasound probe (2 cm diameter Ti-horn, 20 kHz, 500 W) immersed directly in the reaction solution. The sonication was conducted without cooling so that the temperature of the reactant mixture increased gradually (~353 K) and the colour of the solid solution changed slowly from brownish to yellow.

The resultant yellow solid ($VOPO_4 \cdot 2H_2O$ phase), was then recovered by using centrifuge technique and subsequently washed sparingly with acetone and oven dried at 373 K for 24 h and denoted as DS15, DS30, DS45, DS60, DS90 and DS120.

DS120 was chosen to further react to become $VOHPO_4 \cdot 0.5H_2O$ by reflux with isobutyl alcohol (1 g/20 mL from BDH) at 393 K for 21 h and the blue solid sample was centrifuged out from the solvent and dried in oven at 373 K for 24 h. The precursor obtained was calcined in reaction flow of 0.75 % *n*-butane/air mixture for 18 h at 733 K to generate the active catalyst denoted as VPDS120.

Catalysts characterization: The total surface area of the catalysts were measured by the Brunauer-Emmett-Teller (BET) method using nitrogen adsorption at 77 K. This was done by a Sorptomatic 1990 Series, Thermo Fischer-Scientific instrument.

The bulk chemical composition was determined by using a sequential scanning inductively coupled plasma-atomic emission spectrometer (ICP-AES) (Perkin-Elmer Emission Spectrometer model plasma 1000). The average oxidation numbers of vanadium in the sample bulk was determined by redox titration following the method of Niwa and Murakami[2]. X-ray diffraction (XRD) analysis was carried out by using a Shimadzu diffractometer model XRD 6000. The electron microscopy techniques were used to obtain the information on the morphology and size of the samples by LEO 1455 Variable Pressure scanning electron microscope (SEM). The morphology was studied at an accelerating voltage of 30 kV. The particles were attached on an aluminium stub by using double-sided tape. The preparation was covered by using a thin layer of gold coating by using BIO-RAD Sputter Coater. The SEM micrographs were recorded by using a digital camera at various magnifications.

The particle size of the samples was examined using LEO 912AB energy filter transmission electron microscope (TEM) with an acceleration voltage of 120 keV.

H_2-TPR analysis was performed using ThermoFisher Scientific TPDRO 1100 apparatus equipped with a thermal conductivity detector (TCD). The experiment was done by following the thermal conductivity of the outlet stream with TCD when raising the temperature of the fresh catalysts was raized from ambient to 1223 K at 10 K/min in a H_2/Ar stream.

The oxidation of *n*-butane was carried out at 673 K with GHSV = 2400 h^{-1} in a fixed-bed microreactor with a standard mass of catalyst (250 mg). *n*-Butane and air were fed to the reactor *via* calibrated mass flow controllers to give a feedstock composition of 1.0 % *n*-butane in air. The products were then fed *via* heated lines to an on-line gas chromatograph for analysis. The reactor comprised a stainless steel tube with the catalyst held in place by plugs of quartz wool. A thermocouple was located in the centre of the catalyst bed.

RESULTS AND DISCUSSION

X-ray diffraction (XRD): The XRD patterns (Fig. 1) of the vanadyl phosphate dihydrate obtained, $VOPO_4 \cdot 2H_2O$, *via* sonochemical synthesis in different duration of time are perfectly matched with the standard $VOPO_4 \cdot 2H_2O$ (JCPDS File No. 36-1472). The main characteristic peaks at 2θ = 11.9°, 23.9° and 28.7° are corresponding to (001), (002) and (200) planes, respectively.

The sonochemical synthesis process with different duration of time that produce vanadyl phosphate dihydrate, $VOPO_4 \cdot 2H_2O$, basically does not cause any changes, in terms of the basic matrix of the $VOPO_4 \cdot 2H_2O$ phase, which could be evidenced from the standard that being provided by the JCPDS. Hence, this further prove that no peaks of any other phases were detected indicating the high purity of the $VOPO_4 \cdot 2H_2O$ produced through this sonochemical synthesis technique that have been drastically reduced the synthesis time to only 15 min compared to the conventional reflux method that consumed the synthesis time up to 24 h.

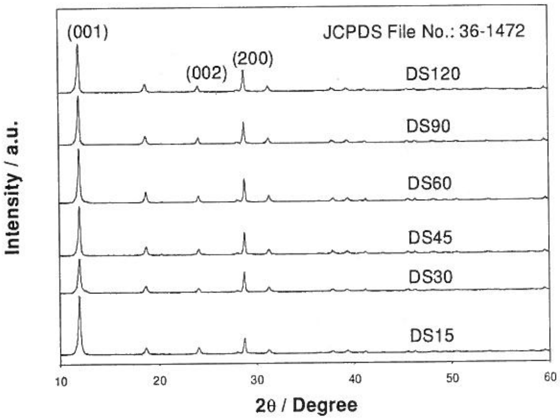

Fig. 1: XRD patterns of sonochemical synthesized vanadyl phosphate dihydrate (DS15-DS120)

The XRD patterns of the VPO catalysts synthesized using vanadyl phosphate dihydrate that undergo the sonochemical synthesis for 2 h, DS120, compared to the bulk VPO catalyst that synthesized through the reduction of vanadyl phosphate dihydrate using conventional reflux method are shown in Fig. 2. Both VPO catalyst produced are very similar and characteristic of $(VO)_2P_2O_7$ phase with (020), (204) and (221) lines at 22.9°, 28.4° and 29.9°, respectively. No other VPO phase could be detected by the XRD analysis for both of the catalyst synthesized. However, the trace amount of V^{5+} species was detected in redox titration analysis which was not detected in the XRD.

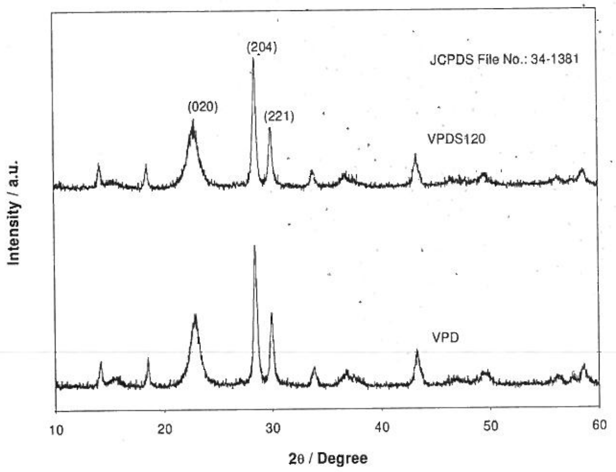

Fig. 2: XRD patterns of VPDS120 and VPD catalyst synthesized

BET Surface area measurements and chemical analysis: VPO catalyst prepared *via* sonochemical synthesized $VOPO_4 \cdot 2H_2O$ gave similar surface area to the reference catalyst. Chemical analysis obtained from ICP-AES (Table-1) indicated that the respective bulk P/V atomic ratios for VPD and VPDS120 are in the desired optimal P/V atomic ratio range of 1.0 to 1.2, which is well-agreed with the findings by Horowitz and co-workers[3]. These values were generally accepted to be the optimum ratio in preparing the active component $(VO)_2P_2O_7$ for the maleic anhydride production[4,5]. Slightly access P/V atomic ratio[6,7] helps in avoiding the oxidation of V^{4+} in $(VO)_2P_2O_7$.

TABLE-1

SPECIFIC BET SURFACE AREA, CHEMICAL PROPERTIES, AVERAGE VANADIUM VALENCE AND PERCENTAGES OF V^{4+} AND V^{5+} OXIDATION STATES PRESENT IN VPD AND VPDS120 CATALYSTS

Catalysts	Specific BET Surface area (m^2/g)	Atomic ratio P/V	Oxidation of the Vanadium		
			V^{4+} (%)	V^{5+} (%)	V_{av}
VPD	25.0	1.08	71	29	4.29
VPDS120	26.0	1.03	89	11	4.11

The average oxidation state of vanadium of 4.29 and 4.11 were obtained for VPD and VPDS120, respectively. Sonochemical synthesis method drastically decreases the formation of V^{5+} phase ($VOPO_4$) from 29 to 11 %. In other words, sonochemical synthesis technique promote the formation of more V^{4+} phase *i.e.* $(VO)_2P_2O_7$, which are responsible for the partial oxidation of *n*-butane towards maleic anhydride[4,5].

Scanning electron microscope (SEM): Fig. 3. shows the SEM micrograph of $VOPO_4 \cdot 2H_2O$ prepared through conventional reflux method. The morphology of $VOPO_4 \cdot 2H_2O$ produced consist of large platelet particles that are stacked to each other to form layered material. This is in agreement with the results obtained by other research groups[8-10].

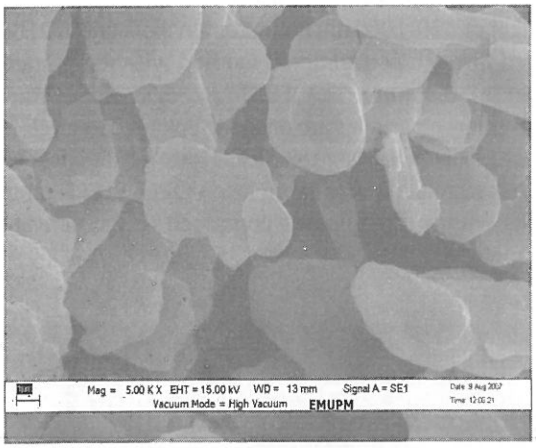

Fig. 3.: SEM micrograph of VOPO4 (with 10000× magnification)

The morphologies of $VOPO_4 \cdot 2H_2O$ produced by undergo the sonochemical synthesis technique were shown in Fig. 4. The microstructure of the $VOPO_4 \cdot 2H_2O$ obtained through this technique are smaller with irregular shape compared to the conventional method. However, for the $VOPO_4 \cdot 2H_2O$ that undergo the sonochemical technique for 120 min. Fig. 4f. shows a much more uniform plate-like structure and stack to each other to form a layered structure. The uniformity with narrow size distribution in DS120 morphology which could benefit the catalytic properties is the reason it has been chosen to further synthesized into VPO catalyst.

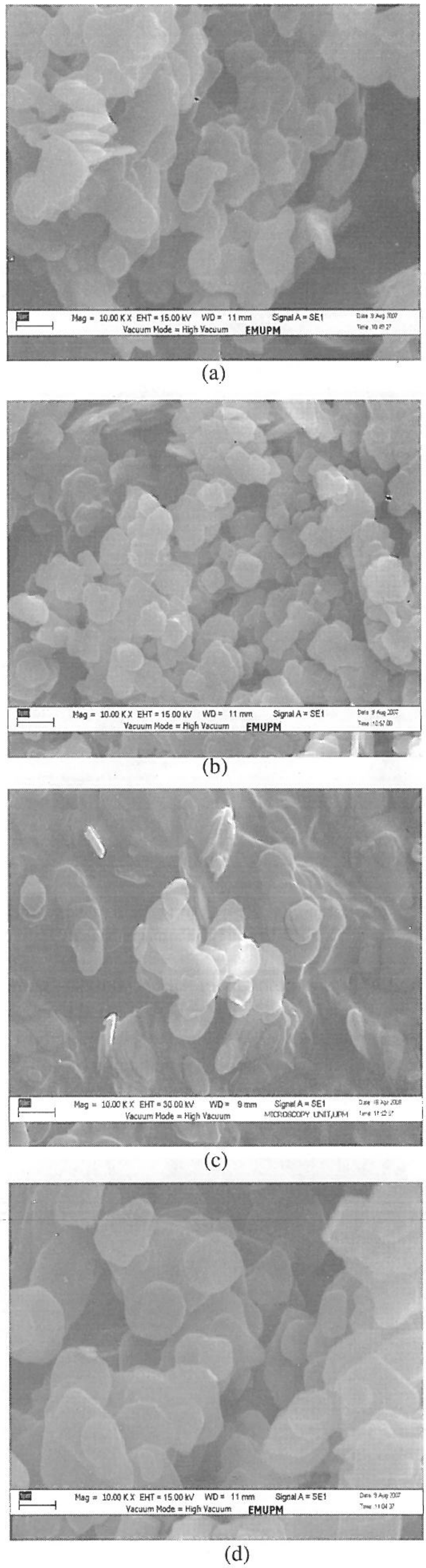

(a)

(b)

(c)

(d)

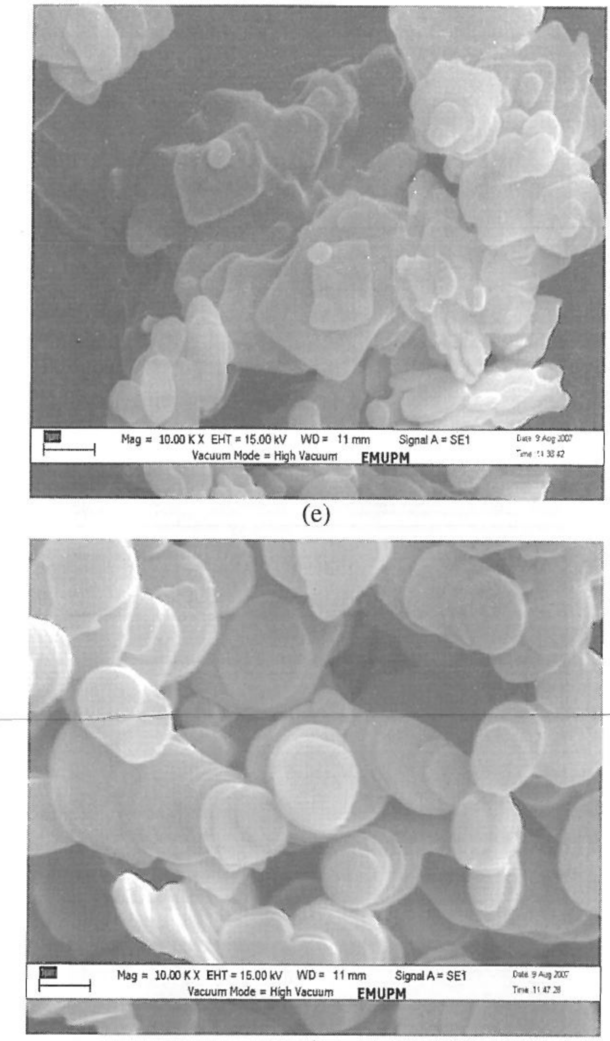

(e)

(f)

Fig. 4.: SEM micrograph of (a) DS15, (b) DS30, (c) DS45, (d) DS60, (e) DS90 and (f) DS120 (with 10000× magnification)

The morphology shown for VPO catalyst obtained *via* reduction of $VOPO_4{\cdot}2H_2O$ route which formed using conventional reflux method (VPD) is more disorganized (Fig. 5) compared to the catalyst obtained *via* reduction of $VOPO_4{\cdot}2H_2O$ which undergo the sonochemical synthesis for 2 h (VPDS120) (Fig. 6).

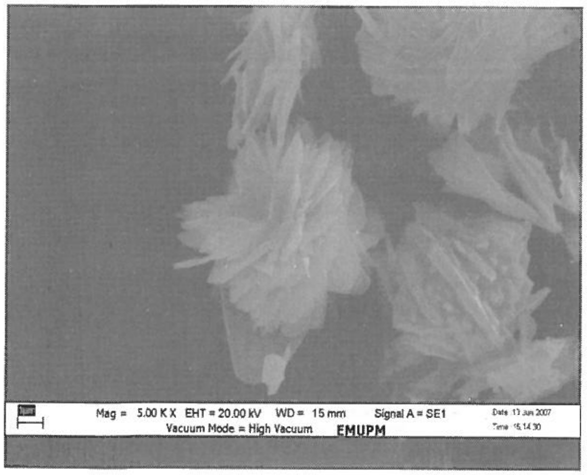

Fig. 5: SEM micrograph of VPD (with 5000× magnification)

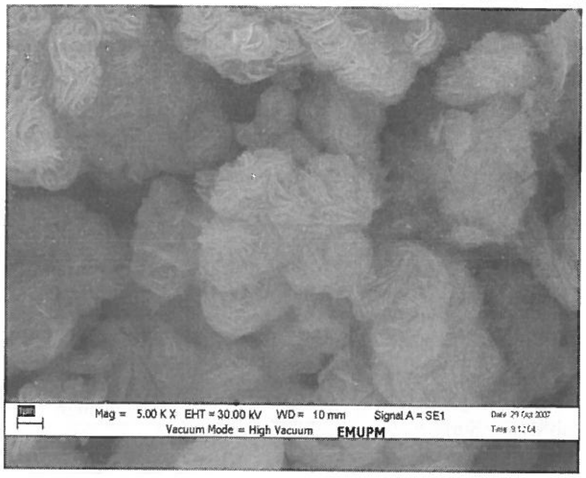

Fig. 6: SEM micrograph of VPDS120 (with 5000 × magnification)

The crystal plates of VPDS120 catalyst obtained *via* the sonochemical synthesis of $VOPO_4{\cdot}2H_2O$ had arranged themselves to form sphere rosebud structures with diameters of ~2720 nm, thickness of platelet of ~30 nm and quite uniform sizes compared to VPD catalyst that form rosette-shape clusters with larger diameters (~8150 nm) and thicker platelets (~320 nm). These rosebud structures, which made up of $(VO)_2P_2O_7$ aggregates are preferentially exposing the (100) crystal plane[11] are therefore less oxidizable[12].

Transmission electron microscope (TEM): Fig. 7. shows the particle size of the $VOPO_4{\cdot}2H_2O$ synthesized through sonochemical synthesis technique with different duration of time were examined by using transmission electron microscope. The TEM images show that the sonochemical synthesized $VOPO_4{\cdot}2H_2O$ are indeed consist of sub-micron particles with diameters of 420-1060 nm compared to the $VOPO_4{\cdot}2H_2O$ that prepared through conventional method with the particle size of about 0.1-0.3 mm[13]. This TEM images also confirmed that this sub-micron particles are unstable and tend to agglomerate with each other to form larger particle. However, the sonochemical synthesis technique is able to produce $VOPO_4{\cdot}2H_2O$ sub-micron particles within few minutes compared to the conventional reflux method.

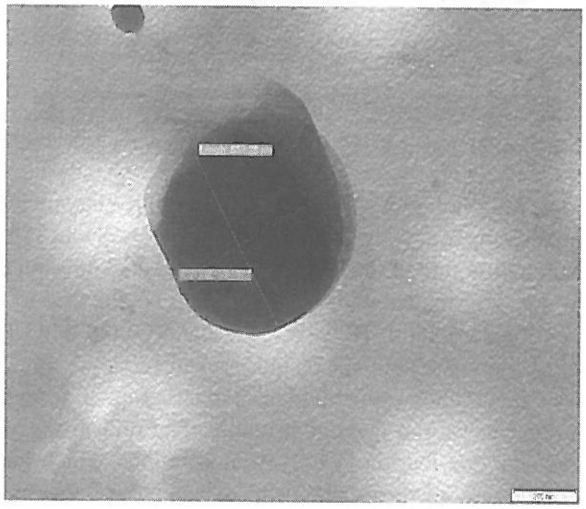

(a) ~500 nm

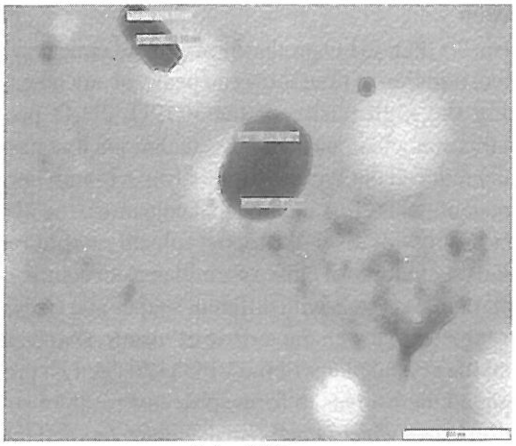

(b) ~400 nm

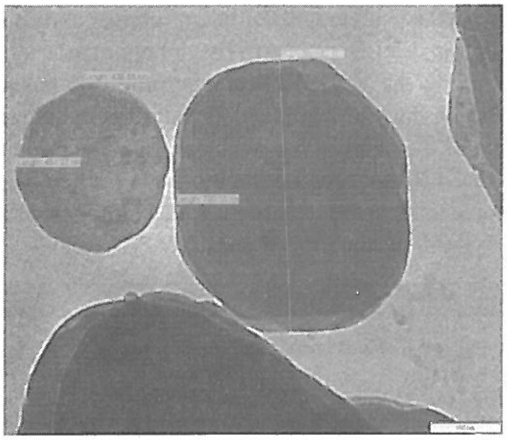

(c) ~450 nm

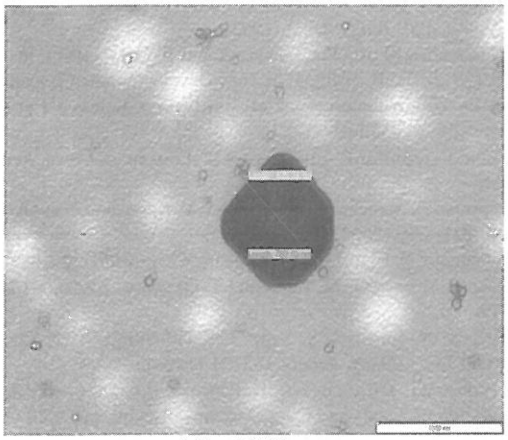

(d) ~1000 nm

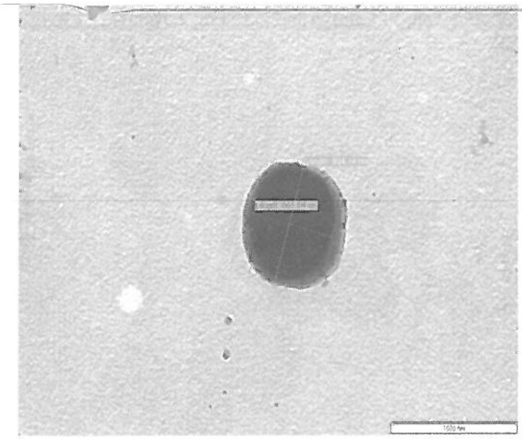

(e) ~700 nm

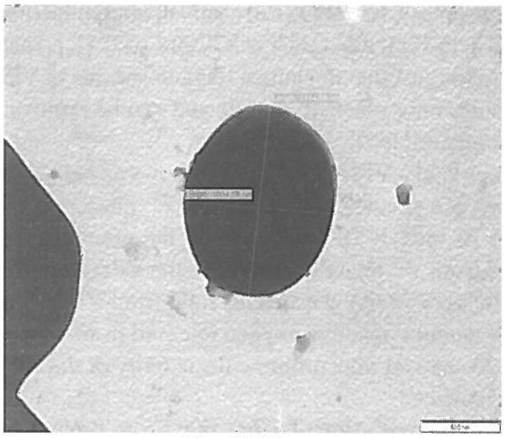

(f) ~1000 nm

Fig. 7. TEM micrograph of (a) DS15, (b) DS30, (c) DS45, (d) DS60, (e) DS90 and (f) DS120

Temperature programmed reduction (TPR in H_2/Ar): H2-TPR profiles and the total amount of oxygen removed from the catalysts synthesized are shown in Fig. 8. and Table-2, respectively. VPD catalyst gave a characteristic of two reduction peaks occurred at 893 and 1045 K, which correspond to the reduction of V^{5+} and V^{4+} phases, respectively. The area of both peaks assigned to the removal of lattice oxygen species associated with the corresponding phases. The amount of oxygen removed from both peaks is 0.19×10^{21} and 1.35×10^{21} atom g^{-1}, respectively with an oxygen ratio removed from V^{5+}/V^{4+} of 0.14.

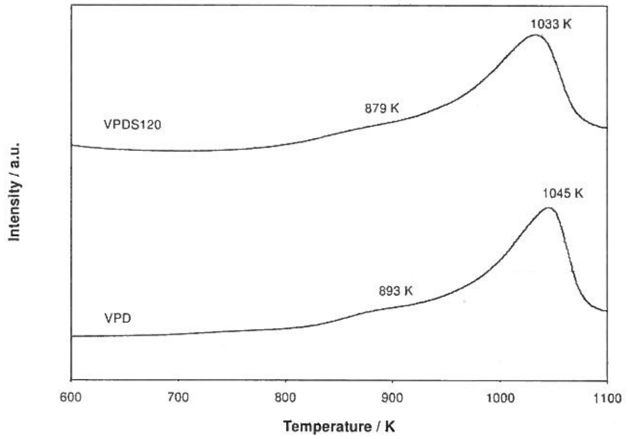

Fig. 8. TPR profiles for VPD and VPDS120 catalysts

TABLE-2

TOTAL AMOUNT OF OXYGEN REMOVED FROM VPD AND VPDS120 CATALYSTS BY REDUCTION IN H_2/AR

Catalyst (Peak)	T_{max} (K)	Oxygen Atom Removed ($\times 10^{-3}$ mol g^{-1})	Oxygen Atom Removed ($\times 10^{21}$atomsg^{-1})	Ratio for oxygen removal of V^{5+}/V^{4+}
VPD				
1	893	0.31	0.19	0.14
2	1045	2.25	1.35	
Total oxygen atoms removed		2.56	1.54	
VPDS120				
1	879	0.30	0.18	0.13
2	1033	2.37	1.43	
Total oxygen atoms removed		2.67	1.61	

Interestingly, for VPDS120 catalyst, both reduction peaks occurred at lower temperature at 879 and 1033 K, respectively. This may suggest that the lattice oxygen species in VPDS120 catalyst are more reactive, mobile and can be removed more easily compared to the VPD catalyst.

Remarkably, VPDS120 catalyst shows an increased (6 %) of the oxygen species removed from V^{4+} phase with a slight decrease of 0.01×10^{21} atom g^{-1} on the amount of oxygen removed from V^{5+} phase compared to the VPD catalyst (Table -2). These give an oxygen species ratio from V^{5+}/V^{4+} of 0.13. A higher amount of active oxygen released from V^{4+} phase for VPDS120 catalyst may promote the activity of the catalyst as reported earlier[14].

Catalytic oxidation of *n*-butane: From Table-3, conventional VPD catalyst achieved 25 % of *n*-butane conversion and MA selectivity, which makes a total of 6.3 % of MA yield. Interestingly, 61 % of *n*-butane conversion rate was achieved with VPDS120 catalyst which means a total of 36 % increment was observed for the *n*-butane conversion. However, VPDS120 catalyst shows a slight decrement (15 %) in MA selectivity which makes a total of MA yield decreased to 6.1 % compared to VPD catalyst.

TABLE-3
CATALYTIC PERFORMANCE OF SONOCHEMICAL SYNTHESIZED VPDS120 AND BULK VPD CATALYSTS FOR OXIDATION OF *n*-BUTANE

Catalysts	*n*-Butane conversion (%)	Product selectivity (%)			MA yield (%)
		MA	CO	CO_2	
VPD	25.0	25.0	57.0	18.0	6.3
VPDS120	61.0	10.0	1.0	89.0	6.1

From the catalytic evaluation, VPDS120 catalyst shows an improvement in the *n*-butane conversion. This may be majorly due to the different morphology obtained for the VPDS120 and VPD catalyst produced whereby VPDS120 catalyst had arranged the particles to form sphere rosebud structure with uniform sizes which has smaller diameters and thickness of platelets that directly increase the active site of the catalyst for oxidation of *n*-butane compared to VPD catalyst. Moreover, VPDS120 catalyst contain more V^{4+} percentage which directly lead to the increment of the total amount of active oxygen released from V^{4+} phase (O^{-}-V^{4+} pair) at lower temperature in H_2-TPR analysis whereby, it indicated VPDS120 catalyst contain more reactive and mobile lattice oxygen species in the V^{4+} phase compared to VPD catalyst that directly contribute to increment of the percentage of *n*-butane conversion which is in agreement with the catalytic evaluation performed.

Conclusion

All the $VOPO_4{\cdot}2H_2O$ produced *via* sonochemical synthesis in different duration of time shows no peaks of any other phases indicating the high purity of the $VOPO_4{\cdot}2H_2O$ produced through this sonochemical synthesis technique that have been drastically reduced the synthesis time to only 15 min compared to the conventional reflux method that consumed the synthesis time up to 24 h. Moreover, the topographical morphologies of VPD catalyst exhibited a close resemblance structure, consisting of plate-like crystals with different shapes and sizes, which were arranged into the characteristic of rosette-shape clusters. However, the crystal plates of the VPDS120 catalyst produced had arranged themselves to form sphere of rosebud structure with uniform sizes which contain smaller diameters and thickness of platelets. Interestingly, VPDS120 catalyst shows a drastically increment in the percentage of *n*-butane conversion compared to conventional VPD catalyst. This phenomenon occurred majorly due to the VPDS120 catalyst produced has smaller diameters and thickness of platelets that directly increase the active site of the catalyst for oxidation of *n*-butane. Furthermore, VPDS120 catalyst contain more V^{4+} percentage which directly lead to the increment of the total amount of active and mobile oxygen attached to V^{4+} phase (O^{-}-V^{4+} pair).

REFERENCES

1. U.R. Pillai, E. Sahle-Demessie and R.S. Varma, *Appl. Catal. A: Gen.*, **252**, 1 (2003).
2. M. Niwa and Y. Murakami, *J. Catal.*, **76**, 9 (1982).
3. H.S. Horowitz, C.M. Blackstone, A.W. Sleight and G. Teufer, *Appl. Catal.*, **38**, 193 (1988)
4. B.K. Hodnett, *Catal. Rev. Sci. Eng.*, **27**, 373 (1985).
5. G. Centi, *Catal. Today*, **16**, 5 (1993).
6. M. Guilhoume, M. Roullet, G. Pajonk and B. Grzybowska, in eds.: J.C. Volta, P. Ruiz and B. Delmon, In: New Developments in Selective Oxidation by Heterogeneous CatalysisElsevier Science Publication, Amsterdam, p. 255 (1992).
7. G. Centi, F. Trifirò, J.R. Ebner and V.M. Franchetti, *Chem. Rev.*, **88**, 55 (1988).
8. N. Hiyoshi, N. Yamamoto, N. Ryumon, Y. Kamiya and T. Okuhara, *J. Catal.*, **221**, 225 (2004).
9. N. Yamamoto, N. Hiyoshi and T. Okuhara, *Chem. Mater.*, **14**, 3882 (2002).
10. T. Nakato, Y. Furumi, N. Terao and T. Okuhara, *J. Mater. Chem.*, **10**, 737 (2000).
11. C.J. Kiely, A. Burrows, S. Sajip, G.J. Hutchings, M.T. Sananes, A. Tuel and J.C. Volta, *J. Catal.*, **162**, 31 (1996).
12. F. Cavani and F. Trifirò, in eds.: G. Poncelet, P. Grange and P.A. Jacobs, Preparation of Catalysts IV, Amsterdam: Elsevier, pp. 1-25 (1995).
13. N.G. Park, K.M. Kim and S.H. Chang, *Electrochem. Commun.*, **3**, 553 (2001)
14. Y.H. Taufiq-Yap, Y. Kamiya and K.P. Tan, *J. Nat. Gas. Chem.*, **15**, 297 (2006).